

# Real-time electrical and morphological characterizations of gas sensing $\text{Ti}(\text{Pc})_2$ devices under working conditions

Amanda Generosi<sup>a,\*</sup>, Barbara Paci<sup>a</sup>, Valerio Rossi Albertini<sup>a</sup>, Paolo Perfetti<sup>a</sup>,  
Anna Maria Paoletti<sup>b</sup>, Gianna Pennesi<sup>b</sup>, Gentilina Rossi<sup>b</sup>, Ruggero Caminiti<sup>c</sup>

<sup>a</sup> *Istituto di Struttura della Materia-Area di Ricerca di Tor Vergata, Via del Fosso del Cavaliere 100, 00133 Roma, Italy*

<sup>b</sup> *Istituto di Struttura della Materia-Area di Ricerca di Montelibretti, Via Salaria Km. 29.5, CP10 Monterotondo Stazione, Roma, Italy*

<sup>c</sup> *Dipartimento di Chimica, Università "La Sapienza" di Roma e sezione INFN, P.le A. Moro 5, 00185 Roma, Italy*

Received 12 March 2007; received in revised form 18 July 2007; accepted 23 July 2007

Available online 6 August 2007

## Abstract

The present study investigates the response of  $\text{NO}_2$  gas sensing devices, based on bis(phthalocyaninato)titanium thin films, by combined electrical and time-resolved energy-dispersive X-ray reflectometry (EDXR) analysis. Samples of various thicknesses were exposed to a  $\text{NO}_2$  gas flux and their electrical response was recorded, during interaction with the oxidising molecules. At the same time, the changes induced in the film thickness and roughness, produced by the "breathing like" mechanism, which characterized the diffusion of the gas in the film bulk, were monitored by EDXR. Comparing the two results, the first direct correspondence between the morphological changes and the electrical response of the sensor was found. This also demonstrates that the morphological characteristics of the films are actually related to their sensing behaviour and can therefore be used, as an alternative to the electrical response, to follow the gas–film interaction process.

© 2007 Elsevier B.V. All rights reserved.

**Keywords:** EDXR; Gas sensors;  $\text{TiPc}_2$ ;  $\text{NO}_2$ ; Morphology

## 1. Introduction

Intensive studies have been carried out on metal phthalocyanines (MPcs) as molecular electrical conductors and semiconductors [1–4] due to the fact that they generally acquire semiconducting (charge carriers) properties when doped with electron acceptors or donors. This behaviour, which is of great importance for numerous technological applications [5,6], is closely connected to their structural and electronic properties. Among the more recently synthesized "stapled-sandwich species", bis(phthalocyaninato)titanium(IV) [7],  $[\text{Ti}(\text{Pc})_2]$ , is intensively investigated [8,9]. Indeed this molecule, like monomeric phthalocyanines, but unlikely from intrinsic semiconducting bis(phthalocyanines) [10], is insulating when undoped ( $\sigma < 10^{-12} \Omega^{-1} \text{cm}^{-1}$ ); its conductivity increases very much when exposed to  $\text{NO}_2$ , while it is almost insensitive to oxygen, it exhibits a short response time, a good reversibility

and a remarkable selectivity, so that gases such as  $\text{NO}$ ,  $\text{SO}_2$ ,  $\text{CO}$ , and  $\text{NH}_3$  present in the air and the air itself do not produce any effect [11]. As a matter of fact, its capability of undergoing relevant and reversible electrical/optical changes upon exposure to gases such as  $\text{NO}_2$  makes this molecule one of the most interesting  $\text{M}(\text{Pc})_2$  for sensing applications [12–14], and it has therefore been studied by both optical or conductometric techniques.

Studies on phthalocyanine–gas interaction mechanism allowed to attribute the conduction mechanism to the formation of a charge-transfer complex formed between a phthalocyanine donor and an  $\text{NO}_2$  acceptor, the charge carriers being the holes produced in the phthalocyanine matrix [15,16].

Furthermore, many evidences suggest that also the film deposition process strongly affects the sensing properties and this influence differs from MPcs to MPcs, depending on the chemical nature of the phthalocyanine and on the film texture deriving from the evaporation process. These observations, indicate that the phthalocyanine film morphology plays a fundamental role in the response to gas exposure [17–20] and that the precise control of the organization and thickness of the films may enhance the performance of the device.

\* Corresponding author. Tel.: +39 0649934146; fax: +39 0649934153.  
E-mail address: [Amanda.Generosi@ism.cnr.it](mailto:Amanda.Generosi@ism.cnr.it) (A. Generosi).

Several theoretical models [21,22] have been developed to correlate for instance the electrical behaviour of MPCs films to the diffusion mechanisms. The morphological response of the material to the gas has recently been used for explaining the  $\text{NO}_2$ - $\text{Ti}(\text{Pc})_2$  interaction mechanism and the morphological reversibility of the sensor, and its behaviour as a function of the gas concentrations was investigated [19,23]. Indeed, the  $\text{NO}_2$  diffuses into the film lattice and this process is favoured by a reversible surface rearrangement, being a thermodynamic process independently on the gas concentration [20]. However, no simultaneous recording of the electrical response and the change of morphology upon exposure to  $\text{NO}_2$  in order to find the correlation between these two processes have been carried so far. In the present work, the first joint electrical/morphological measurements on the gas sensor devices are reported. In order to experimentally correlate the electrical behaviour to the evolution of the morphological parameters, a series of thin  $\text{Ti}(\text{Pc})_2$  films were studied during their exposure to the gas flux.

## 2. Experimental

The  $\text{Ti}(\text{Pc})_2$  was synthesized following the method described in a previous paper [7] and, then, deposited as thin films (50–110 nm) on interdigital electrodes (Fig. 1a) by evaporation in an Edwards A306 coater, at 350 °C and at  $10^{-6}$  Torr, the substrate being at room temperature. Film thickness was monitored by an Edwards FTM5 film thickness monitor (density 1.428). The electrode consisted of 40 interdigital pairs of gold fingers, 20  $\mu\text{m}$  wide and spaced 20  $\mu\text{m}$  from each other. The interdigital electrodes, as a substrate, are essential to measure conductivity changes on weak conducting phthalocyanine (e.g.,  $10^{-12}$  S/cm), in order to avoid high voltages that would cause electrochemical degradation at the phthalocyanine–electrode interface.

The experimental equipment used for the joint electrical and morphological measurements consisted of a plastic cell, used as a device chamber, which was placed in the centre of the X-

ray reflectometer. In the plastic cell,  $\text{NO}_2$  gas was introduced at a concentration of 50 ppm in  $\text{N}_2$ , while the electric current through the electrode was monitored, providing the real-time resistivity value. At the same time, a sequence of X-ray patterns, representing the intensity reflected by the film, was collected. From the analysis of the patterns, the morphological parameters, namely the thickness and surface roughness of the film, can be deduced and correlated to the resistivity measurements.

X-ray reflectometry is a technique which is sensitive to films morphology at the angstrom resolution [23]. The detailed theory is reported elsewhere [24] but, at a first approximation, it can be described using the classical reflection/refraction law, i.e. Snell rule. The rule implies that the reflected X-ray intensity is a function of the momentum transferred from the radiation to the atomic electrons of the film,  $\mathbf{q}$ . Since  $|\mathbf{q}| = aE \sin \vartheta$  [25] (where  $a$  is a constant =  $1.014 \text{ \AA}^{-1}/\text{keV}$ ,  $E$  the radiation energy and  $\vartheta$  is the scattering angle), the  $q$ -scan can be carried out either by scanning  $\vartheta$  or by scanning  $E$ . The former method is the traditional angular dispersive mode; the latter is the energy dispersive X-ray reflectivity (EDXR) mode [26], which makes use of a continuum spectrum radiation, for example the Bremsstrahlung of an X-ray tube, in which the scattering angle is kept fixed.

Therefore, while the measurement of the electric resistivity was performed in a standard way (see the following description), the ED technique, used for the reflectivity measurements, somehow differed from the conventional approach. The EDXR method was preferred because it simplified the experimental geometry, allowing the simultaneous collection of electrical and morphological information. Indeed, in EDXR, the scanning of the reciprocal space was performed electronically by an energy sensitive X-ray detector, rather than by mechanical movements of the reflectometer arms. In this way, all problems connected with the variable geometry, such as the change of the X-ray beam footprint size onto the film, were prevented.

A computer-assisted apparatus with an HP Digital Multimeter (HP 3458A) connected to the electrode, as shown schematically in Fig. 1b, was used to record current as a function of time. dc current measurements were performed (100 nA on 5.5 digits, maximum sensitivity 1 pA) applying 0.8 V to the  $\text{Ti}(\text{Pc})_2$  device and collecting the signal by averaging it over 5 min time intervals.

## 3. Results and discussion

All measurements were performed under room conditions, the main interest being to investigate the electrical and morphological behaviours under real working conditions, i.e. in the presence of air and relative humidity.

The first step in the experimental procedure was a preliminary current versus time measurement, while fluxing a 50 ppm  $\text{NO}_2$  gas into the experimental chamber containing the device. The conductivity variation of the  $\text{Ti}(\text{Pc})_2$  film during exposure to  $\text{NO}_2$  and its electrical reversibility upon chemical and physical treatments (i.e. illumination, thermal treatments, exposure to reductive agents) was already reported in the literatures [13,14] but, in the present case, it was carried out at a higher time resolution, in order to discriminate between the two subsequent

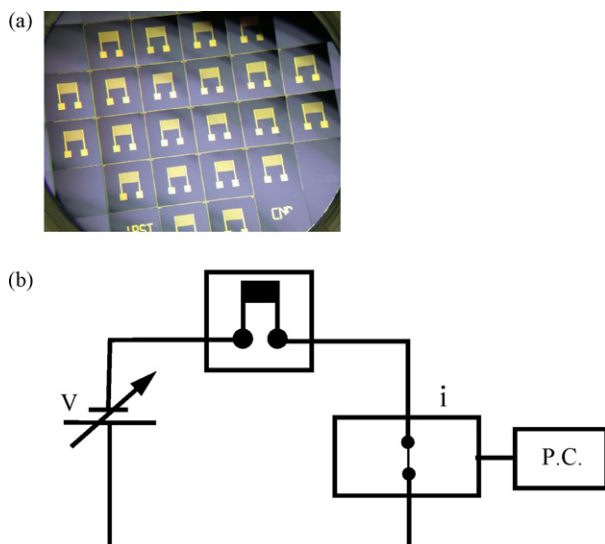
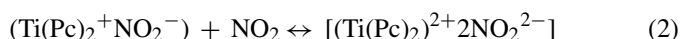
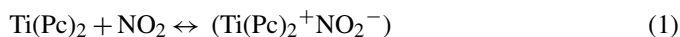


Fig. 1. (a) Image of the interdigitated substrates used to deposit  $\text{Ti}(\text{Pc})_2$ . (b) Sketch of the electric circuit used to perform the current vs. time measurements.

oxidation processes, which occurred between the thin film and the gas. This objective has been reached as shown in Fig. 2 where the two processes are well distinct. This result further strengthens the mechanism already proposed [10] where the charge carriers, generated by the gas interaction, were well identified as two chemical species (each one characterized by different conductivity and colour) which were in equilibrium during the process, as follows:



The presence of  $\text{NO}_2$  gas produces in this system two oxidised species, monocation and bication, responsible for the conductivity increase. Despite both species are present, the monocationic species are the main responsible for the conduction process.

With reference to Fig. 2a, the first conductivity peak corresponds to the formation of the monocation species  $(\text{Ti(Pc)}_2^+ \text{NO}_2^-)$ . As the reaction proceeds, the equilibrium is shifted towards the second process and the dicationic species  $[(\text{Ti(Pc)}_2)^{2+} 2\text{NO}_2^{2-}]$ , which are not as conductive as the monocationic, coexist with the latter, inducing a slight decrease in intensity (Fig. 2b). This dynamic redox equilibrium, which takes place between the two cationic phthalocyanine species, corresponds in the conductivity curve to the plateau following the first peak.

Finally, as the mobility of the charge carriers decreases, the conductivity decreases. At this point, the  $\text{NO}_2$  stream was interrupted and  $\text{N}_2$  (180 nmol/s) alone was fluxed onto the sample (Fig. 2c). According to Eq. (2), the removal of  $\text{NO}_2$  from the experimental chamber shifts the overall redox equilibrium back to Eq. (1) due to the fact that the monocationic species  $(\text{Ti(Pc)}_2^+ \text{NO}_2^-)$  become more numerous. As a consequence, a second conductivity maximum is reached, followed by a very slow decrease of the conductivity due to the progressive dis-

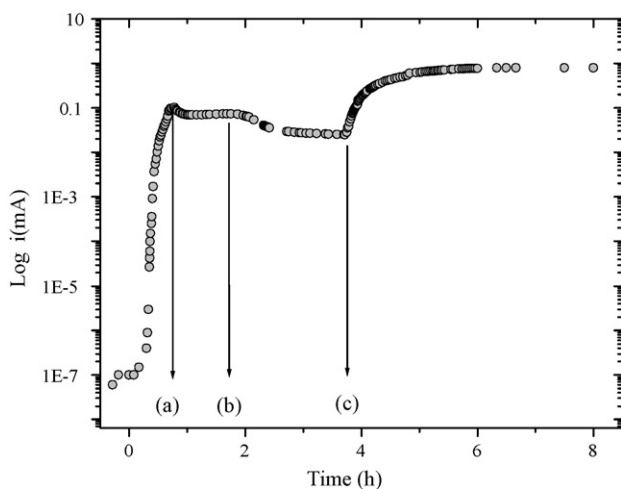


Fig. 2. Variation of the current intensity through a 50 nm thick  $\text{TiPc}_2$  film as a function of time when exposed to a mixture of  $\text{NO}_2/\text{N}_2$  (20 nmol/s and 180 nmol/s, respectively) and then, to pure  $\text{N}_2$ . (a) The first peak corresponds to the formation of the monocationic species  $(\text{Ti(Pc)}_2^+ \text{NO}_2^-)$ . (b) Equilibrium between the monocationic  $(\text{Ti(Pc)}_2^+ \text{NO}_2^-)$  and bicationic  $[(\text{Ti(Pc)}_2)^{2+} 2\text{NO}_2^{2-}]$  species. (c) Introduction of pure  $\text{N}_2$  to remove  $\text{NO}_2$ .

appearance of the charge carriers. Once the reproducibility of the conductometric behaviour with this new experimental set-up was verified, the chamber was placed in the X-ray reflectometer. In this way, it was possible to carry out joint time-resolved morphological/electrical measurements on a series of  $\text{Ti(Pc)}_2$  films, with different nominal thickness, under the same experimental conditions as already described.

Sequences of reflectivity patterns were collected (the integration time of each pattern being 9 min) while the oxidising gas was being fluxed into the chamber. Simultaneously, a current versus time measurement was performed, as described previously. The time sampling period was chosen to balance the competing needs of reducing the noise/signal ratio, while maintaining an accurate sampling of the whole oxidising process.

In Fig. 3, a sequence of reflectivity patterns, collected upon a 110 nm (nominally) thick  $\text{Ti(Pc)}_2$  film, is shown as a function of the scattering parameter  $q$  ( $\text{\AA}^{-1}$ ) and of time. Kiessig fringes [27] (oscillations due to the interference between the X-ray beams reflected at the film surface and at the film/substrate interface) are clearly visible. The arrow (Fig. 3) connecting the minima of the third oscillation shows how, as the exposure to the  $\text{NO}_2$  molecules proceeds, the oscillation frequency increases. The shift of the oscillations towards lower  $q$  values indicates that a morphological change is taking place during the gas–film interaction, i.e. the film is becoming thicker. The raw estimation of the film thickness  $d$  can be performed using the simplified formula  $d \approx 2\pi/\Delta q$  ( $\text{\AA}$ ), where  $\Delta q$  is the oscillation period expressed in  $\text{\AA}^{-1}$ , and a more accurate calculation was obtained by a Parratt fit of each spectrum [28]. In this way, the evolution of the diffusion process was monitored, as illustrated in Fig. 4a, through the real-time observation of the film thickening (“swelling”)

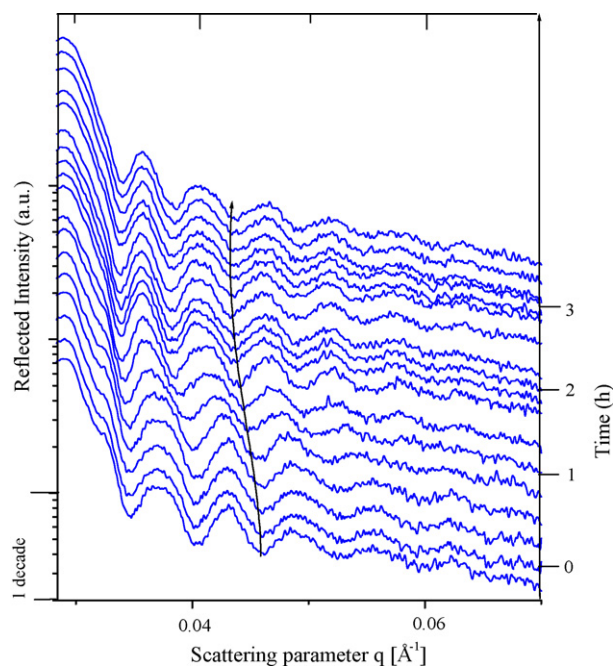


Fig. 3. Sequence of reflectivity patterns collected as a function of the scattering parameter and of the  $\text{NO}_2$  exposure time. The arrow, connecting the third oscillation minima, underlines the increasing frequency of the fringes as a function of time.

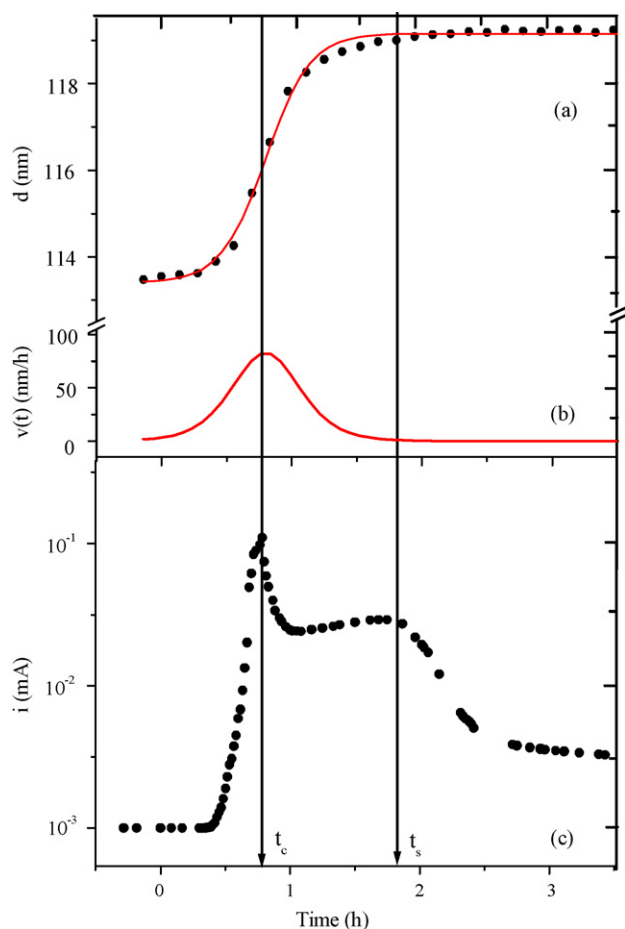


Fig. 4. (a) Evolution of the thickness parameter ( $d$ ) of a 110 nm nominally thick  $\text{Ti(Pc)}_2$  film as a function of time ( $t$ ) during exposure to a 50 ppm  $\text{NO}_2$  gas flux. (b) The derivative of  $d$  vs.  $t$ . (c) The current vs. time, collected simultaneously to the morphological evolution shown in (a). The vertical arrows shows that both processes are characterized by the same characteristic time  $t_c$  and by the same saturation time  $t_s$ .

due to bulk diffusion of the  $\text{NO}_2$  molecules into the  $\text{Ti(Pc)}_2$  matrix.

The overall  $d$  versus  $t$  curve can be well fitted by a Boltzmann sigmoid. The time derivative of this fit (Fig. 4b) enables the characteristic time  $t_c$ , corresponding to the maximum speed of diffusion of  $\text{NO}_2$  into the film bulk, to be calculated easily. In Fig. 4, the first stage of the electrical response is compared with the morphological changes occurring in the film in the same time interval. The information obtained by comparison of the two sets of data evidences a direct correspondence between the characteristic time of bulk diffusion and that of the electrical response. Indeed, the electrical peak signal related to the formation of the monocationic species (at  $t_c$  in curve c) corresponds to the maximum  $\text{NO}_2$  diffusion speed (curve b), the characteristic time  $t_c$  being  $45 \pm 15$  min.

This result represents the first experimental observation of the direct correlation existing between the morphological change in the film induced by interaction with the gas and the electrical response of the film. Moreover, when the oxidation reaction between  $\text{Ti(Pc)}_2$  and  $\text{NO}_2$  is driven further, the species in Eqs. (1) and (2) tend towards an equilibrium. As soon as equilibrium

is reached, the diffusion process of the gas molecules in the film bulk also approaches saturation, at  $t = t_s = 105 \pm 15$  min in Fig. 4. Indeed, at this point, the conduction sites are saturated, the mobility of the charge carriers decreases and the conductivity reaches a plateau at a level slightly higher than the starting value. The film thickening also approaches its asymptotical value.

The exact correspondence between the two characteristic times of the bulk diffusion and the electrical response was verified by further measurements performed on films of different thickness. Indeed, the fact that the overall increase in thickness is proportional to the initial thickness of the film and that the characteristic time of the morphological change process scales with the film initial thickness, indicates that the gas–film interaction is a pure bulk diffusion process. The same characteristic was also observed in the electrical response.

#### 4. Conclusions

In conclusion, these first joint measurements show the direct correlation between the morphological response of the gas sensing device, and the chemical interaction occurring at a molecular level between  $\text{Ti(Pc)}_2$  and  $\text{NO}_2$ . Finally the role of morphology has been clearly associated to the electrochemical response of the device and its relevance was experimentally proven.

The results demonstrate the possibility of retrieving information on the gas–film interaction mechanism, by measuring two independent observable simultaneously, such as electronic and structural properties, under real working conditions. This validates the use of the EDXR non-conventional technique as a complementary investigation tool when gas–film interactions are monitored.

#### Acknowledgments

The authors are grateful to Mr. Marco Luce for the technical support for the in situ electrical measurements and to Mr. A. Casling for his critical reading of the manuscript.

#### References

- [1] J.R. Ferraro, J.M. Williams, Introduction to Synthetic Electrical Conductors, Academic Press, Florida, 1987, p. 219.
- [2] M.Y. Ogawa, J. Martinsen, S.M. Palmer, J.L. Stanton, J. Tanaka, R.L. Green, B.M. Hoffman, J.A. Ibers, The (phthalocyaninato)copper iodide complex  $\text{Cu(pc)I}$ : a molecular metal with a one-dimensional array of local moments embedded in a “Fermi sea” of charge carriers, *J. Am. Chem. Soc.* 109 (1987) 1115–1121.
- [3] T. Inabe, J.G. Gaudiello, M.K. Moguel, J.W. Lyding, R.L. Burton, W.J. McCarthy, C.R. Kannewurf, T.J. Marks, Cofacial assembly of partially oxidized metallomacrocycles as an approach to controlling lattice architecture in low-dimensional molecular “metals”. Probing band structure–counterion interactions in conductive  $[\text{M}(\text{phthalocyaninato})\text{O}]_n$  macromolecules using nitrosonium oxidants, *J. Am. Chem. Soc.* 108 (1986) 7595–7608.
- [4] M. Hanack, U. Keppeler, H.-J. Schulze, Iodine-doped bridged phthalocyaninatoiron(II) and ruthenium(II) compounds, *Synth. Met.* 20 (1987) 347–356.
- [5] G. Guillaud, J. Simon, J.P. Germain, Metallophthalocyanines: gas sensors, resistors and field effect transistors, *Coord. Chem. Rev.* 178–180 (1998) 1433–1484.
- [6] L. Valli, Phthalocyanine-based Langmuir–Blodgett films as chemical sensors, *Adv. Colloid Interface Sci.* 116 (2005) 13–44.

- [7] C. Ercolani, A.M. Paoletti, G. Pennesi, G. Rossi, A. Chiesi-Villa, C. Rizzoli, Two phthalocyanine units ‘stapled’ by carbon–carbon  $\sigma$  bonds in a new sandwich-type molecule: {5,5';19,19'-bi[phthalocyaninato (2<sup>-</sup>)]titanium(IV)}. Synthesis, X-ray crystal structure, and properties, *J. Chem. Soc., Dalton Trans.* 1 (1990) 1971–1978.
- [8] A. Capobianchi, C. Ercolani, A.M. Paoletti, G. Pennesi, G. Rossi, A. Chiesi-Villa, C. Rizzoli, Interligand carbon–carbon sigma-bond breaking and repair in a ‘‘stapled’’ bis(phthalocyaninato)titanium complex. Synthesis, characterization, and electrical conductivity properties of oxidation products of bis(phthalocyaninato)titanium(IV) and bis(phthalocyaninato)tin(IV) and X-ray crystal structure of [Pc<sub>2</sub>Ti](I3)0.66, *Inorg. Chem.* 32 (1993) 4605–4611.
- [9] A. Capobianchi, A.M. Paoletti, G. Pennesi, G. Rossi, S. Panero, Electrochromism in sandwich-type diphtalocyanines: electrochemical and spectroscopic behaviour of bis(phthalocyaninato)titanium(IV) (Ti(Pc)<sub>2</sub>) film, *Synth. Met.* 75 (1995) 37–42.
- [10] M. Tromoter, R. Even, J. Simon, A. Dubon, J.Y. Laval, J.P. Germain, C. Maleysson, A. Pauly, H. Robert, Lutetium bisphthalocyanine thin films for gas detection, *Sens. Actuator B: Chem.* 8 (1992) 129–135.
- [11] F. Baldini, A. Capobianchi, A. Falai, A.A. Mencaglia, G. Pennesi, Reversible and selective detection of NO<sub>2</sub> by means of optical fibres, *Sens. Actuator B: Chem.* 74 (2001) 12–17.
- [12] A. Capobianchi, A.M. Paoletti, G. Pennesi, G. Rossi, Effect of nitrogen dioxide on titanium bisphthalocyaninato thin films, *Sens. Actuator B: Chem.* 48 (1998) 333–338.
- [13] F. Baldini, A. Capobianchi, A. Falai, G. Pennesi, A new sandwich-type diphtalocyanine as a potential optical transducer for NO<sub>2</sub> detection, *Sens. Actuator B: Chem.* 51 (1998) 176–180.
- [14] A. Capobianchi, A.M. Paoletti, G. Pennesi, G. Rossi, Italian Patent RM 2000 A000028.
- [15] H. Tian, K.-C. Chen, Diffusion behaviour of charge carriers in thin films of phthalocyanines, *Dyes Pigments* 27 (1995) 191–196.
- [16] M.E. Azim-Araghi, D. Campbell, A. Krier, R.A. Collins, Electrical conduction mechanisms in thermally evaporated lead phthalocyanine thin films, *Semicond. Sci. Technol.* 11 (1996) 39–43.
- [17] J.C. Hsieh, C.J. Liu, Y.H. Ju, Response characteristics of lead phthalocyanine gas sensor: effects of film thickness and crystal morphology, *Thin Solid Films* 322 (1998) 98–103.
- [18] V. Rossi Albertini, A. Generosi, B. Paci, P. Perfetti, G. Rossi, A. Capobianchi, A.M. Paoletti, R. Caminiti, Time resolved energy dispersive X-ray reflectometry measurements on phthalocyanine gas sensor films upon working, *Appl. Phys. Lett.* 82 (22) (2003) 3868–3870.
- [19] A. Generosi, B. Paci, V. Rossi Albertini, P. Perfetti, A.M. Paoletti, G. Pennesi, G. Rossi, A. Capobianchi, R. Caminiti, Experimental evidence of a two steps absorption/desorption process in ruthenium phthalocyanine gas sensing films by in situ energy dispersive X-ray reflectometry, *Appl. Phys. Lett.* 86 (2005) 114106–114108.
- [20] A. Generosi, B. Paci, V. Rossi Albertini, P. Perfetti, A.M. Paoletti, G. Pennesi, G. Rossi, R. Caminiti, Evidence of a rearrangement of the surface structure in Ti(Pc)<sub>2</sub> sensors induced by the interaction with nitrogen oxides molecules, *Appl. Phys. Lett.* 87 (1) (2005) 181904–181906.
- [21] Y.H. Ju, C. Hsieh, C.J. Liu, The surface reaction and diffusion of NO<sub>2</sub> in lead phthalocyanine thin film, *Thin Solid Films* 342 (1999) 238–243.
- [22] R. Tongpool, S. Yoriya, Kinetics of nitrogen dioxide exposure in lead phthalocyanine sensors, *Thin Solid Films* 477 (2005) 148–152.
- [23] A. Generosi, B. Paci, V. Rossi Albertini, P. Perfetti, G. Rossi, A.M. Paoletti, G. Pennesi, R. Caminiti, Morphological variations as nonstandard test parameters for the response to pollutant gas concentration: an application to ruthenium phthalocyanine sensing films, *Appl. Phys. Lett.* 88 (2006) 104106–104108.
- [24] V. Rossi Albertini, B. Paci, A. Generosi, Energy dispersive X-ray reflectometry as a unique laboratory tool for investigating morphological properties of layered systems and devices, *J. Phys. D: Appl. Phys.* 39 (2006) 461–486.
- [25] A. Generosi, V. Rossi Albertini, G. Rossi, G. Pennesi, R. Caminiti, Energy dispersive X-ray reflectometry of the NO<sub>2</sub> interaction with ruthenium phthalocyanine films, *J. Phys. Chem. B* 107 (2003) 575–579.
- [26] R. Caminiti, V. Rossi Albertini, The kinetics of phase transitions observed by energy-dispersive X-ray diffraction, *Int. Rev. Phys. Chem.* 18 (1999) 263–299.
- [27] H. Kiessig, Reflectivity oscillations at grazing incidence in thin Ni films, *Ann. Phys.* 10 (1931) 769–788.
- [28] L.G. Parratt, Surface studies of solids by total reflection of X-rays, *Phys. Rev.* 95 (1954) 359–369.

## Biographies

**Amanda Generosi** received Laurea degree in chemistry and PhD degree in materials science from the University of Rome La Sapienza. She got a post doctoral fellowship at the I.S.M., C.N.R., in Rome, working in collaboration with the X-ray Spectroscopy Laboratory. Her main activities cover the structural/morphological investigations of layered materials as basis for gas sensing devices and for renewable energy sources (plastic solar cells, fuel cells).

**Barbara Paci** received Laurea degree in physics, summa con laude, and PhD in physics. Responsible of the ‘‘devices for Kyoto protocol application CNR-RST-research activity’’ focusing on gas sensors and organic solar cells, at I.S.M., C.N.R. in Rome. *Interests:* molecular physics, organic films for non-linear optics, amorphous solids, electronic and electrochemical devices. *Expertise:* X-ray (laboratory and synchrotron), neutron, linear and non-linear optical (pump and probe) techniques and computer simulations.

**Valerio Rossi Albertini** received Laurea degree in physics, PhD in materials science. Responsible of the ‘‘X-ray Spectroscopy Laboratory’’ at I.S.M., C.N.R. in Rome. *Interests:* molecular physics, liquids and amorphous solids, electronic and electrochemical devices. *Expertise:* X-ray (laboratory and synchrotron) and neutron techniques, IR spectroscopy, computer simulations and ab initio calculations.

**Paolo Perfetti** was born in Terni, Italy, on 20 April 1942. He received Laurea degree in physics, he is the director of the Institute of Structure of Matter of CNR since 1989. *Interests:* solid state physics, surface science in particular using direct and inverse photoemission, LEED, AUGER analysis and synchrotron radiation.

**Anna Maria Paoletti** had the PhD in chemical sciences, is currently senior scientist at the Institute of Structure of Matter of CNR in the research field of Molecular Materials with Non-conventional Properties, her work includes the study of phthalocyanine compounds material for optoelectronics and photonics.

**Giovanna Pennesi** graduated in chemistry, is currently senior scientist at the Institute of Structure of Matter of CNR in the research field of Molecular Materials with Non-conventional Properties, her work attained mostly at the utilisation and characterization of phthalocyanine compounds as thin films in optical and conductimetric gas-sensors for the environmental monitoring.

**Gentilina Rossi** graduated in chemistry is senior scientist at the Institute of Structure of Matter of CNR and leads the Group of Molecular Materials with Non-conventional Properties in the same Institute; her research interests are in the field of synthesis, characterization and development of new phthalocyanine compounds useful for application in electronic or optical devices.

**Ruggero Caminiti** graduated in chemistry at the University of Rome. He is currently full professor of *physical chemistry* at Rome’s University ‘‘La Sapienza’’ (since 2001) being the responsible of the Laboratory of X-ray Diffraction. *Interests:* EDXD and EDXR, biomembrane models and disordered systems.